''Ordered'' structure in ionic dilute solutions: Dendrimers with univalent and bivalent counterions

Atsuyuki Ohshima,[1] Toshiki Konishi,[1,*] Junpei Yamanaka,[2] and Norio Ise[1,†]
[1]*Central Laboratory, Rengo Co., Ltd., 186-1-4, Ohhiraki, Fukushima-ku, Osaka 553-0007, Japan*
[2]*Faculty of Pharmaceutical Sciences, Nagoya City University, 3-1, Tanabe, Mizuho, Nagoya 467-8603, Japan*
(Received 14 March 2001; published 24 October 2001)

As an intermediate sample of ionic solutes between colloidal particles (macroions) and simple electrolyte ions, we made small-angle x-ray scattering (SAXS) measurements for aqueous solutions of poly(amido amine) dendrimers of three generations (G4, G7, and G10). The SAXS curves of univalent acid solutions showed a single scattering peak, as observed for synthetic macroions. The peak position was dependent on the dendrimer concentration but independent not only of the acid concentration (degree of protonation) but also of the counterion species. The effective charge density of the dendrimer determined by conductivity measurements was found to be insensitive to the acid concentration and the counterion species. The nearest neighbor interparticle distance $2D_{exp}$ calculated from the peak position of the structure factor of G7 and G10 was obviously smaller, though slightly, than the average interparticle distance $2D_0$ calculated from molecular weights and concentrations of dendrimers, implying that acid solutions of dendrimers formed the two-state structures by the attractive force. The ultra-small-angle x-ray scattering curve for the hydrochloric acid solution did not show an upturn, which indicates the existence of large scale structural inhomogeneities such as localized ordered structures, probably due to the weak attraction and hence less clear distinction of the ordered and disordered regions. For sulfuric acid solutions, clear scattering peaks were not observed. The bivalent counterions were more strongly associated with the dendrimer ions than the univalent ones. The resulting low charge number of the dendrimers with the bivalent counterion was confirmed directly by the conductivity measurements. These observations confirm that the counterion-mediated attraction does exist even with the univalent counterions and point out that the frequently advanced claim that the effective potential is essentially repulsive with univalent counterions while attraction appears with bivalent counterions is not necessarily correct. It is noted that the intensity of the counterion-mediated attraction in dendrimer solutions is dictated by both the effective charge density and the effective charge number, in contrast with macroionic solutions or colloidal dispersions in which only the effective charge density appeared to be important.

DOI: 10.1103/PhysRevE.64.051808 PACS number(s): 83.80.Rs, 61.10.Eq, 61.20.Qg, 66.10.Ed

I. INTRODUCTION

Dilute solutions of ionic polymers show a single broad peak in small-angle x-ray scattering (SAXS) [1,2] and small-angle neutron scattering (SANS) profiles [3], when the concentration of coexisting salt is low and the molecular weight is high enough. Although various interpretations of the peak have been proposed, we have attributed the peak to an ''ordered'' arrangement of macroions. One of the most unexpected features is the presence of microscopic inhomogeneity in the macroion distribution, namely the two-state structure, in other words the coexistence of ordered regions and disordered (Brownian) particles [4]. Such an inhomogeneity was inferred from the observation that the Bragg spacing between macroions ($2D_{exp}$) was generally smaller than the average interparticle spacing $2D_0$ calculated from the macroion concentration. Consistently, dynamic light scattering (DLS) study revealed two relaxation modes in macroscopically homogeneous polyelectrolyte solutions at low salt conditions [5]. These observations were confirmed by microscopic investigation of colloidal particle dispersions [6], albeit definitely with different time and space scales, ruling out the validity of the above-mentioned various interpretations of the scattering peak. The two-state structure was photographed for latex dispersions by us [6,7] and 14 years later by Larsen and Grier [8].

The above observations were made for synthetic macroions, biological macroions and colloidal particles [2]. An outstanding macroscopic inhomogeneity, namely coexistence of particle-rich liquid phase and particle-poor vapor phase, was observed for polystyrene-based latex in light water, below a critical particle concentration by Arora's group [9]. Under the density-matched condition (D_2O-H_2O mixture), Yoshida *et al.* found that the two phases were transformed into the coexistence of liquid structure and a large number of microscopic voids (regions without particles) at the corresponding concentrations [10]. Recently, Gröhn and Antonietti investigated spherical polyelectrolyte microgels in dilute aqueous solutions by static light scattering [11]. This microgel study covers macroions over 1 decade of radii (7–70 nm) and showed also the inequality relationship $2D_{exp}<2D_0$ at lower concentrations, where macroscopic phase separation was again noticed. In the present paper we report our x-ray scattering study on another polyelectrolyte system, namely ionic dendrimers. Our main purpose is to examine whether the structural inhomogeneity mentioned above can be ob-

*Corresponding author.
†Present address: 23, Nakanosaka, Kamigamo, Kita-ku, Kyoto 603-8024, Japan.
Email address: norioise@ip.media.kyoto-u.ac.jp

served also for these rather undeformable polyelectrolytes (radii ranging from 2 nm to 7 nm) and also to discuss the structural properties in terms of the charge number and the charge density. Unlike in most of the previous papers, in which these parameters were treated as adjustable, we determine the analytical charge number or density and the effective charge number or density by independent measurements. Our approach certainly reduces the number of uncertain factors and serves making the argument more straightforward. We also investigate the influence of counterions in the structural behavior. In most of earlier work using colloidal particles, the protons were counterions. To understand the nature of the electrostatic interaction correctly, variation of the counterions was desirable but practically difficult from an experimental point of view on colloidal particles so far used.

Dendrimer is a spherical branched polymer whose architecture is highly controlled three-dimensionally [12]. The dendrimer has many special features, for example, (1) it has multifunctional end groups, (2) the molecular weight distribution is very narrow, (3) detailed molecular design is possible, and (4) the solution viscosity is lower than those of linear polymers with same molecular weight. In the past decade, many kinds of the dendrimer, which have different initiator core and branches, are synthesized [13] and intensive studies on practical use of dendrimers as a new functional material are made, for example, the use of nanocapsules [14], the drag delivery system [15,16] using the inner space of the dendrimer, and so on. Among them, poly(amido amine) (PAMAM) dendrimer, which is composed of ethylenediamine as the initiator core and the copolymer of ethylenediamine and methyl acrylate as the branch, has primary amine groups at each branch end and tertiary amine groups at each branching point, so that it behaves as a globular polyelectrolyte in acid solutions. Besides the above-mentioned applications, the PAMAM dendrimer can be used as very convenient model compound for investigating polyelectrolyte systems, because of their regulated spherical shape, well-defined molecular weight, and distribution, and well-defined analytical charge number.

II. EXPERIMENT

A. Materials

Dendrimers used in this study were the fourth, seventh, and tenth generation ''Starburst® PAMAM Dendrimer'' samples purchased from Dendritech™ Inc. (Michigan, USA) and/or Aldrich. They were named G4, G7, and G10, respectively. These samples were dialyzed by cellulose tube (Spectrum, Spectra/Por® Membrane MWCO: 1000) against water for several days with monitoring by conductivity measurements, and then purified by the ion-exchange resin (Bio-Rad, AG® 1-X8 Resin), which was purified by washing with Milli-Q water and subsequent ultrasonic treatment at 40 °C. Table I gives their characteristics.

Water used in this study was purified by a Milli-Q system and the conductivity was below 0.6 $\mu S\,cm^{-1}$.

TABLE I. PAMAM dendrimers used in this study.

Sample	$M(10^4)$[a]	The number of end groups
G4	1.4	64
G7	11.6	512
G10	93.3	4096

[a]Molecular weight (calculated).

B. Small-angle x-ray scattering (SAXS) and ultra-small-angle x-ray scattering (USAXS)

A Kratky-U-slit type SAXS instrument was used with a one-dimensional position sensitive proportional counter (Rigaku Corporation, Tokyo, Japan) and the x-ray generator RU-300 (50 kV×280 mA, Rigaku Co.). Water and aqueous solutions of hydrochloric acid, perchloric acid, hydrobromic acid, iodic acid, and sulfuric acid were used as solvent. Measurements were made for dendrimer solutions with dendrimer weight fraction w being from 0.01 to 0.10 and acid concentrations from 0.05 to 0.5 N at room temperature (ca. 25 °C). The SAXS data were desmeared by the method of Lake-Schmidt [17,18].

The ultra-small-angle x-ray scattering (USAXS) apparatus employed was constructed by the Bonse-Hart optics and described earlier [19].

C. Electric conductivity

Electric conductivity measurements were performed as follows [20]. To aqueous solution of the dendrimer, aqueous acid solution was added dropwise, and the electric conductivity was monitored continuously by a conductivity meter DS-14 (HORIBA Ltd., Kyoto, Japan) with a cell of the cell constant of 1.01 cm^{-1} at 25 °C. Aqueous acid solutions were the same as in the SAXS measurements.

III. RESULTS

A. SAXS

Figure 1 shows SAXS curves for aqueous solutions of dendrimers G4, G7, and G10 at fixed w. The ordinate is the relative intensity of scattered x rays $I(q)$ and the abscissa is the magnitude of the scattering vector $q[=(4\pi/\lambda)\sin\theta; 2\theta$: scattering angle; λ: wavelength of incident x ray (= 0.154 nm)]. The curves are shifted vertically. Solid curves are theoretical particle scattering function $P(q)$ calculated by assuming that dendrimers are uniform spheres and the number average radii r of G4, G7, and G10 are 2.1, 4.3, and 7.0 nm, respectively. (The ratio s of the standard deviation to r are 0.08–0.10.) The SAXS curves were successfully described by the theoretical curves with $q<2\ nm^{-1}$, and the correspondence seemed to be better for higher generation dendrimers. It indicated that end groups of higher generations were tightly packed, and then shapes of particles were uniform.

Figure 2 shows the acid concentration dependence of SAXS curves for hydrochloric acid solutions of G7 at $w=0.051$. Similar results were obtained for G4 at $w=0.041$, although the graphical presentation was omitted to save

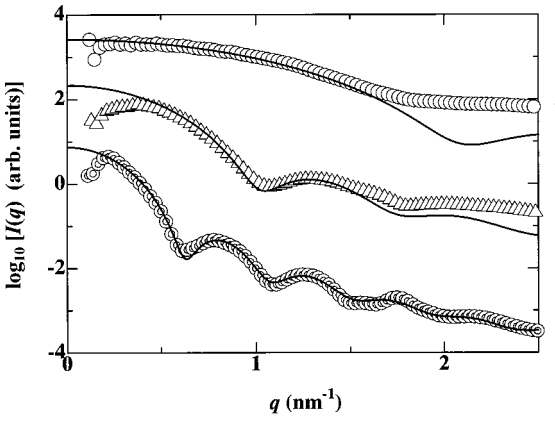

FIG. 1. SAXS curves of aqueous solutions: ○, G4 ($w=0.051$); △, G7 (0.057); ◎, G10 (0.050);—, theoretical curves. (The curves were shifted vertically.)

space. In the present study the amount of added acid (concentration) is represented by α, which is the ratio of the amount of protons to that of the end groups of the dendrimer in the solution and is defined as

$$\alpha = \frac{(\text{equivalent of acid added into solutions})}{(\text{equivalent of the end groups})}. \quad (1)$$

A single scattering peak, which can be distinguished from the maxima of $P(q)$, was observed with $\alpha > 0.3$. The peak

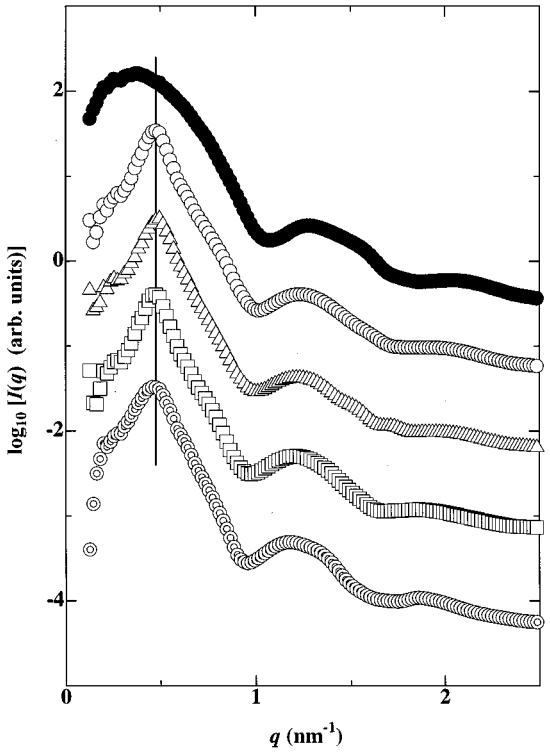

FIG. 2. Acid concentration dependence of SAXS curves for hydrochloric acid solutions of dendrimer G7 at $w=0.051$: ●, $\alpha=0$; ○, 0.5; △, 0.8; □, 1.2; ◎, 1.9, the vertical solid line, the first peak position. (The curves were shifted vertically.)

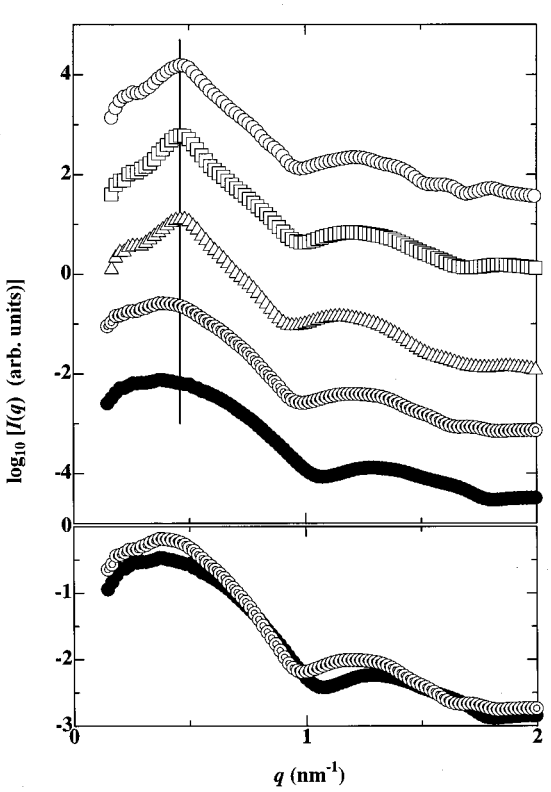

FIG. 3. SAXS curves for several different acid solutions of dendrimer of G7: ○, hydrochloric acid ($w=0.050$, $\alpha=1.0$); □, hydrobromic acid (0.049, 1.0); △, iodic acid (0.050, 1.1); ◎, sulfuric acid (0.050, 1.0); ●, water (0.050, 0) the vertical solid line, the first peak position. (Each curve was shifted vertically, and the inset reproduces the scattering profiles of the sulfate salt and of the water-unneutralized dendrimers on the same scale.)

positions for G4 and G7 were independent of α, and were 0.80 and 0.48 nm^{-1}, respectively. Similar behaviors of hydrochloric acid solutions of PAMAM dendrimers were reported using SANS by Nisato *et al.* [21] and Valachovic [22].

Figure 3 is SAXS curves for four kinds of acid solutions of G7 at $w=0.050$ and $\alpha=1.0$ together with that in water. Clearly a single broad (interparticle) interference peak was observed on the top of the intraparticle scattering factor $P(q)$ as far as the univalent counterions were used. The peak position did not change with the counterion species under the experimental condition employed. On the other hand, the scattering curve for the sulfate system roughly overlapped that in water (namely, unprotonized case), as clear from the inset in the lower part of the plot, showing no interference peak. Practically the same observations, albeit with less sharp peaks, were made for G4. The hydrochloric acid solution of G10 displayed a distinct peak whereas the sulfate solution did not.

Figure 4 shows scattering profiles for G10 at various w's at $\alpha=1.0$. The insensitivity of the profile toward w at large q was clear and the radius r of the dendrimer ions was determined by curve fitting with the theoretical intraparticle scattering for sphere (solid curve) and shown in Table II. The r values at $\alpha \approx 1$ for G4, G7, and G10 were 2.3, 4.5, and 7.1 nm, respectively, which were systematically larger, though

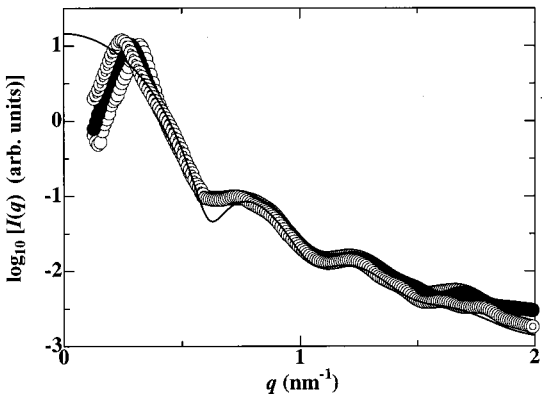

FIG. 4. Dendrimer concentration dependence of SAXS curves for hydrochloric acid solutions of dendrimers G10 at $\alpha=1.0$: ○, $w=0.100$; ●, 0.070; ⊙, 0.050;—, theoretical curve ($r=7.1$ nm). (Each curve was shifted vertically.)

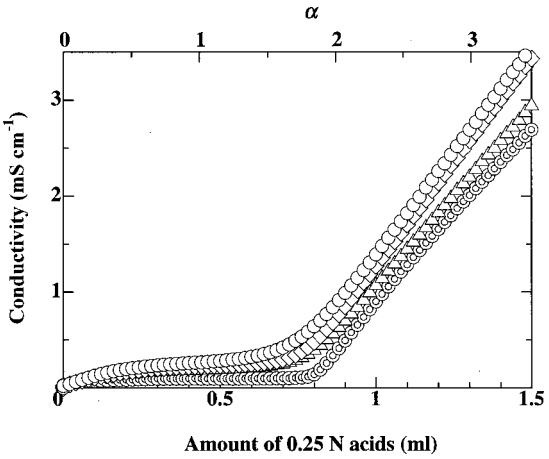

FIG. 5. Electric conductivity titration curves of dendrimer of G4: ○, hydrochloric acid; ◇, perchloric acid; □, hydrobromic acid; △, iodic acid; ⊙, sulfuric acid. (The initial dendrimer concentration and solution volume are 8.21×10^{-5} M and 20.5 ml, respectively.)

slightly, than the corresponding values at $\alpha=0$. This change in r values may be due to the size of hydrogen ions and counterions associated with the dendrimer by neutralization. In the present case, the increase in r may not be due to ionization, because the r value in sulfuric acid solution, where effective charge density is very small (see below) and ionic interaction between the dendrimers is weak (interparticle interference peak being not observed in the inset of Fig. 3), was also larger than in water and was similar to those in more ionized systems such as in hydrochloric acid, perchloric acid, hydrobromic acid, and iodic acid solutions as is seen in Fig. 3. It should be noted that the ionization does not expand the dendrimer ions as much as the prediction based on a Monte Carlo simulation using electrostatic repulsive forces [23]. As often emphasized by us [24–26], the repulsion-only assumption fails in real ionic systems, because it ignores the attraction which ''arises because the repulsion of likes and attraction of unlikes will tend to bring unlikes closer together and pushes likes farther apart'' [27–29].

B. Electric conductivity

Figure 5 shows the electric conductivity of G4 solutions as a function of the amount of added acids. Aqueous solutions (20.5 ml, $w=0.0012$) were titrated with aqueous acid solutions (0.25 N). In the beginning of the titration, the electric conductivity increased gradually with added acids by neutralization. After the completion of the protonation, excess hydrogen ions and counterions increased and hence the electric conductivity of the solutions increased quickly. Similar behavior was observed also for G7 and G10.

For all samples and counterions, the neutralization point observed (breaking point of the conductivity curve) was located at lower $\alpha(=1.8)$ than that expected ($\alpha=2$) for complete ionization of total numbers of primary and tertiary amines. The incomplete ionization might imply that hydrogen ions and counterions could not easily reach all of the tertiary groups because of rather tight structure of the dendrimers.

For sulfate ions as counterions, the conductivity was lower than for univalent counterions and the neutralization point could be noticed more clearly than by the latter. The low conductivity reflects smaller effective charge number of the dendrimer ions with the sulfate ions.

TABLE II. The effective charge density of PAMAM dendrimers at $\alpha=0.6$.

	r (nm)[a]		Z_d[d]		σ_e (μC cm^{-2})[e]		σ_a[f]	σ_e/σ_a	
Sample	Water[b]	Acids[c]	HCl	H_2SO_4	HCl	H_2SO_4	(μC cm^{-2})	HCl	H_2SO_4
G4	2.1	2.3	18	5	4.4	1.1	9.5	0.46	0.12
G7	4.3	4.5	44	11	2.7	0.6_6	19	0.14	0.03_4
G10	7.0	7.1	134	31	3.4	0.7_9	62	0.05_4	0.01_2

[a]Radius.
[b]$\alpha=0$.
[c]$\alpha=1.0$.
[d]The number of the effective charge.
[e]Effective charge density.
[f]Analytical charge density.

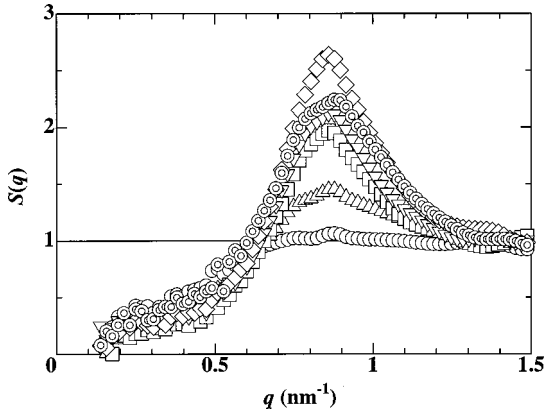

FIG. 6. Acid concentration dependence of the structure factor $S(q)$ for G4 in hydrochloric acid solutions at $w=0.041$: ○, $\alpha=0.1$; △, 0.3; □, 0.6; ▽, 1.0; ◇, 1.5; ⊙, 1.9.

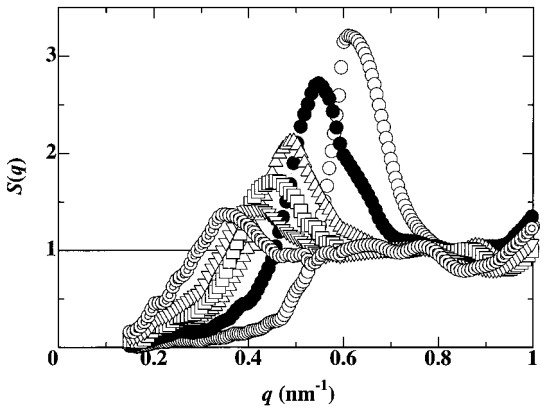

FIG. 7. Dendrimer concentration dependence of the structure factor $S(q)$ for G7 in hydrochloric acid solutions at $\alpha=1.0$: ○, $w=0.100$; ●, 0.070; △, 0.050; □, 0.040; ▽, 0.030; ⊙, 0.020.

IV. DISCUSSION

A. Structure factor

The observed scattering intensity $I(q)$ for solutions of monodisperse hard sphere particles is given using the interparticle interference term, i.e., the structure factor $S(q)$ and the intraparticle scattering factor $P(q)$ by

$$I(q)=AP(q)S(q), \tag{2}$$

where A is a constant. In the present study, $S(q)$ for the univalent counterion systems was evaluated by using $P(q)$ calculated for a uniform sphere [30]. Figure 6 gives the acid concentration dependence of $S(q)$ for hydrochloric acid solutions of G4 at $w=0.041$ and $\alpha=0.1-1.9$. A single broad peak was observed for $\alpha>0.3$, the peak became higher with increasing α up to 1.5, and the peak position was α-independent and 0.87 nm^{-1}. For G7 and G10, also, the SAXS peak position was independent of α and the counterion species, though with different peak positions, as far as α was larger than 0.3. The increase in the peak height with increasing α was earlier noted by Valachovic for ammonia core G8 PAMAM dendrimer using SANS [22]. The drop of the height for $1.5<\alpha<1.9$ would be due to shielding effect by excess acid.

The w dependence of $S(q)$ is shown in Fig. 7 for G7 at $\alpha=1.0$. With decreasing w, the peak became lower and the peak position shifted toward lower q, as was the case with linear polyelectrolytes [2], ionic colloids [31], and polyelectrolyte microgels [11]. The same dependence was observed for ammonia core G8 dendrimer using SANS by Valachovic [22].

The highest peak heights of $S(q)$ observed here were around 3. One of the simple interpretations would be that fairly highly ordered structures of the dendrimer ions were formed in the solutions, though higher order peaks were not observed in the q range covered. The structures would contain large paracrystalline distortion, which allows us to observe only the first order peak, as was demonstrated by Matsuoka *et al.* [32,33].

B. Nearest neighbor distance and localized ordered structures

Assuming that face-centered-cubic (fcc) lattices were formed in the dendrimer-univalent counterion solutions, the nearest neighbor interparticle distance $2D_{exp}$ [$=\sqrt{6}\pi/q_{peak}, q_{peak}$: the first peak position for {111} diffraction of $S(q)$] was estimated from the observed peak position and compared with the average interparticle distance $2D_0$ [$=(\sqrt{2}/2)(4M/N_Ac)^{1/3}$; M: the molecular weight of the dendrimer; N_A: Avogadro's number; c: the mass concentration of the dendrimer]. Figure 8 shows the double-logarithmic plots of $2D_{exp}$ and $2D_0$ vs the number concentration of the dendrimer c' for univalent acid solutions of three generations. Three solid lines in this figure indicate experimental curves connecting data points of $2D_{exp}$ smoothly, and the dashed line indicates $2D_0$. $2D_{exp}$ for each acid solution obeyed a straight line, and the slopes of G4, G7, and G10 were -0.34, -0.33, and -0.36, respectively. We note that $2D_{exp}$ for ammonia core G8 obtained from the SANS results

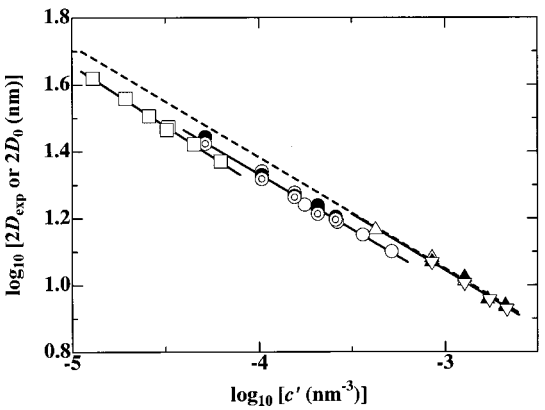

FIG. 8. The dendrimer number concentration dependence of the nearest neighbor interparticle distance $2D_{exp}$: △, G4 (in hydrochloric acid); ▲, G4 (in perchloric acid); ▽, G4 (in iodic acid); ○, G7 (in hydrochloric acid); ●, G7 (in hydrobromic acid); ⊙, G7 (in iodic acid); □, G10 (in hydrochloric acid); − − −, the average distance between dendrimers ($2D_0$) (assuming the face-centered-cubic lattice).

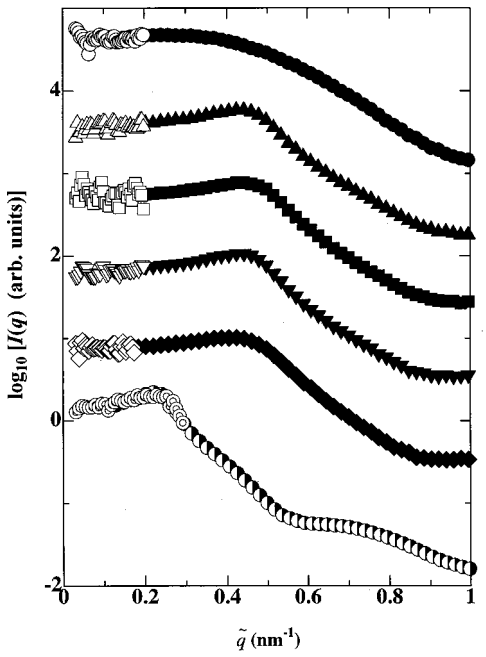

FIG. 9. Smeared USAXS and SAXS curves of G7 and G10 in hydrochloric acid solutions at various α and water. Each curve was shifted vertically, and $\tilde{q}$ is the apparent scattering vector: ○, USAXS (G7 in water); ●, SAXS (G7 in water); △, USAXS (G7, $\alpha=0.5$); ▲, SAXS (G7, 0.5); □, USAXS (G7, 0.8); ■, SAXS (G7, 0.8); ▽, USAXS (G7, 1.2); ▼, SAXS (G7, 1.2); ◇, USAXS, (G7, 1.9); ◆, SAXS (G7, 1.9); ⊙, USAXS (G10, 1.0); ◑, SAXS (G10, 1.0).

by Valachovic [22] was largely consistent with our results, though the slope value was larger than -0.33. We further note that $2D_{\mathrm{exp}}$ for G5 obtained from SANS by Nisato *et al.* [21] with a slope of -0.33 is in good agreement with our results. Though $2D_{\mathrm{exp}}$ of G4 almost agreed with $2D_0$ in the experimental concentration range, those of higher generations were obviously smaller than $2D_0$. It implied that solutions of higher generations formed a two-state structure, namely coexistence of dendrimer-rich and poor regions, indicating the presence of a long-range (counterion-mediated) attractive force between dendrimer ions, as was the case for dilute dispersions of ionic colloidal particles, and for dilute solutions of ionic polymers [24–26] and of ionic polymer microgels [11].

It would be pertinent to comment on the statement by Nisato *et al.* [21] that they did not observe the onset of attractive interaction. Though Nisato *et al.* did not calculate $2D_0$ to compare with $2D_{\mathrm{exp}}$, it is believed based on the agreement shown in Fig. 8 for G4 that their G5 hardly showed the inequality relation, either. Under such a circumstance, their statement is correct. However it is true that the lower generations are not proper samples to finally judge the existence or non-existence of the attraction. They are too weakly charged to result in detectable attraction.

USAXS measurements were performed and the smeared USAXS and SAXS profiles are presented for hydrochloric acid solutions of G7 and G10 at $w\approx 0.05$ in Fig. 9. It is to be noted that the upper limit of structural fluctuation, which can be detected by our USAXS apparatus, is about 8 μm. Nevertheless no upturn down to $q=0.03\,\mathrm{nm}^{-1}$ was observed at $\alpha=0.5-1.9$ of G7 and 1.0 of G10 under our experimental conditions employed. This result is consistent with the SANS measurements by Nisato *et al.* who did not observe the upturn for G5 in a similar range of q [21] but is not in agreement with Valachovic's results [22]. The upturn can be ascribed to the presence of large structural inhomogeneities. Since the $2D_{\mathrm{exp}}/2D_0$ was not very far from unity, it might be plausible that the localized ordered structures of high number densities of dendrimer ions are too large to be detected by the present technique. It might be of some interest to mention here about the upturn in the SANS measurements of polystyrenesulfonate (PSS) solutions [34]. In this case, $2D_{\mathrm{exp}}/2D_0$ was about 0.5 and the radius of gyration R_g derived from the Guinier plot of the upturn was 40 nm to 70 nm, which we ascribed to the size of the localized ordered structure, or the domain size.

C. Effective charge density

Since we are dealing with ionic solutions, and since the interaction therein is mainly long-range electrostatic one, the number of electric charges on solute particles or ions is most crucial in determining the physico-chemical properties of the systems. As a matter of fact, a very slight change in the effective charge number on colloid particles was demonstrated, experimentally and by Monte Carlo simulation, to cause a drastic phase change from liquid state to crystalline (solid) state and from solid state to liquid state [35,36]. On the other hand, it seems that it has been a widely accepted practice in most of previous papers in colloid field to regard the charge number as an adjustable parameter and to introduce ''renormalization of charge'' procedures to reach agreement with chosen theoretical framework, as was pointed out by Yamanaka *et al.* [20]. In the present paper we determine the effective charge density σ_e of dendrimer ions experimentally as was done by Wall and associates for linear polyelectrolytes [37] and by us for colloidal particles [20,38]. Specifically σ_e was estimated as follows. Assuming that the total effective charge number of dendrimers is equal to the total charge number of free counterions, we have

$$Z_d=(Z_c c_c/c_d), \tag{3}$$

where c_c and Z_c are the molar concentration and valency of the free counterions, respectively and c_d and Z_d are the molar concentration of dendrimers and the effective charge number per dendrimer ion, respectively. Since Z_c and c_d are known, c_c needs to be known to obtain Z_d. The electric conductivity of the acid solution of dendrimers (κ) can be written as

$$\kappa=\lambda_c c_c+\lambda_d c_d+\kappa_b, \tag{4}$$

where λ is the limiting equivalent molar conductivity of the ion, and the subscripts d and c stand for dendrimer and counterion, respectively, and κ_b is the background conductivity

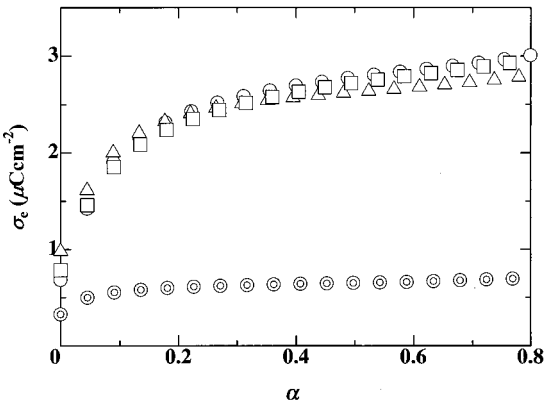

FIG. 10. The acid concentration dependence of the effective charge density σ_c for G7 dendrimers: ○, hydrochloric acid; ◇, perchloric acid; □, hydrobromic acid; △, iodic acid; ◎, sulfuric acid.

due to the water. According to Nernst and Einstein, λ is related to the translational diffusion constant of an ion in dilute solution (D) as

$$D=(RT/F^2)(\lambda/Z^2), \tag{5}$$

where R, T, and F are the gas constant, the temperature, and the Faraday constant, respectively. From Eqs. (3) to (5), we have

$$c_c=\frac{-\lambda_c+\sqrt{(\lambda_c)^2+\dfrac{4D_dF^2}{RTc_d}(Z_c)^2(\kappa-\kappa_b)}}{\left[\dfrac{2D_dF^2}{RTc_d}(Z_c)^2\right]}, \tag{6}$$

where D_d is the diffusion constant of the dendrimers. This quantity can be determined experimentally and the Z_d and hence σ_e can be estimated using the dendrimer radius obtained from the SAXS data. D_d for G4 was determined by DLS while those for G7 and G10 were estimated by the Einstein-Stokes equation using the r values estimated by SAXS measurements.

In the present study, the pH range of the solutions was from about 5 to 9, so that κ_b in Eq. (6) could be neglected. Figure 10 shows the σ_e data of various counterion systems for G7 as a function of α. Quite similar curves were obtained for G4 and G10, though graphical presentation is omitted. Table II gives numerical data of the analytical charge density σ_a and σ_e, together with Z_d. (Note that σ_a is proportional to α.) As seen from Fig. 10, the σ_e values of the univalent counterion systems were not highly dependent on α for $0.3<\alpha<0.8$ and counterion-independent. This result might be related to the observed insensitivity of the peak position of the SAXS curves toward α and the counterion species at a fixed dendrimer concentration (Fig. 2). These insensitivities were also noticed for G4 and G10.

On the other hand, the σ_e values in sulfuric acid solutions (double circle) were lower than those for the univalent counterions. This implies that a larger amount of sulfate ions was strongly condensed on the dendrimer ions than the univalent cases, lowering Z_d and σ_e, and did not contribute to κ. Because of the lower Z_d and σ_e, the interparticle, electrostatic interaction was weakened so that no structure formation and hence no scattering peak could be observed (Fig. 3).

Table II invites further comments. Z_d becomes larger with increasing generation number, while σ_e for each generation is not so different and σ_a naturally becomes larger with increasing generation number. Z_d and σ_e of the bivalent counterions are smaller than those of the univalent counterions.

A few more words appear to be necessary on the influence of the valency of the counterions on the structure formation or the interparticle attraction. We have often come across the assertion that an electrostatic attraction can be observed between like-charged particles or polymeric ions when bivalent counterions are used, but not with univalent counterions [39]. Recently theoretical approach was undertaken by various authors to explain the existence of an attractive interaction between similarly charged macroions. For example Lobaskin *et al.* [40] carried out Monte Carlo simulation for macroions (diameter: 4 nm) of 60 elementary charges and either univalent or bivalent counterions. They found that the effective intermacroion potential was essentially of a Yukawa type with the univalent while an attractive region appeared at short distance (typically 4–5 nm) with the bivalent counterions. It should be reminded that our systems demonstrate the attraction in much longer ranges, for example, at about 20 nm for G10 dendrimers carrying 134 effective charges (the fourth column, Table II), and typically at 1 μm for latex particles of about 10^3 effective charges [25]. Our experimental results in the present paper are not in line with the short-range attraction. Whether macroions or particles form an ordered structure is primarily dictated by the effective charge density or effective charge number of the macroions. The existence of the attraction could be more easily noticed with macroions or particles of higher σ_e as first suggested in our earlier paper (see Table II, Ref. [6]) and redemonstrated in a recent work (see Table 1, Ref. [26]). The counterion valency plays a rather secondary role. At a fixed effective charge of the macroions, needless to say, counterions of higher valency would naturally interact with the macroions more strongly and hence are expected to cause a stronger attraction between the macroions. However, this does not imply that the attraction does not exist with univalent counterions but exists only with multivalent counterions. The attractive interaction with univalent counterions is positively supported by experimental work by us [6,41] and others [42–51] on colloidal particles and polyelectrolytes. In this respect we agree with Ray and Manning [52] when they say that while the attraction is strongly suggested by experiments, some simulation work justifying exclusively repulsive forces with univalent counterions may be in trouble. Whether the attraction with univalent counterions can be detected or not is a matter of the sensitivity of the techniques employed and/or of the quantity under consideration.

An interesting issue arises from comparison of dendrimers and colloidal particles or macroions. As shown in Fig. 8, the difference between $2D_{\mathrm{exp}}$ and $2D_0$ for univalent acid solutions is larger for higher generations than for lower ones.

On the other hand, the σ_e values (the sixth column, Table II) are not so much varied from generation to generation. This insensitivity is rather surprising but is in line with the recent finding in a systematic study by Yamanaka *et al.* [53] that, at a given σ_a for spheres, the σ_e became smaller with increasing sphere diameter. That is also the case in the present work on dendrimers (see the ratio of σ_e and σ_a shown in the last column, Table II). This finding is reasonable because the charge number of a sphere increases with the diameter at a fixed σ_a and so does the interaction with counterions, resulting enhanced counterion association to diminish the effective charge number and density. This factor is counterbalanced by the σ_a becoming larger with increasing generation number (and hence the diameter). The insensitivity of the σ_e for the dendrimers can be understood as a result of these two counteracting effects.

Thus, the important factor in determining the strength of the attraction in question seems to be not σ_e but Z_d (the fourth and fifth columns, Table II), which increased (from 18 to 134) with increasing generation number. However, Z_d $(=31)$ for sulfuric acid cases of G10, for which no scattering peak and hence the structure formation could not be observed, is much larger than that for the hydrochloric acid of G4 $(Z_d=18)$. This result appears to indicate that the interaction between rather small ionic species like dendrimer ions is related both to Z_d and to σ_e, or the ratio of σ_e and σ_a. From analysis of the existing data, it was demonstrated that the interaction between large solutes such as colloidal particles and macroions was primarily governed by σ_e (see Table 1, Ref. [26]). On the other hand, as clear from the Debye-Hükel theory, it is the number of charges on ions that matters in simple electrolyte solutions. This difference is due to the fact that, when two large particles interact with each other, the charges on the local surfaces (areas) of the two particles standing face to face to each other are definitely more influential in determining the interparticle interaction than those on the remote, opposite sides of the two particles. Thus, for large particles or macroions, it is the surface charge density rather than the total number of charge that determines the interparticle interaction. On the other hand, such a situation will not be encountered for small ions, where interionic distance is much larger than the ionic size for dilute solutions. In such cases the total number of charges is a decisive factor. The dendrimers represent an intermediate case between the two extreme cases.

A final comment appears to be necessary on the analysis by Nisato *et al.* using a renormalized mean spherical approximation (RMSA) [21]. They mentioned that the RMSA model ''yielded unphysical results in most cases'' and better agreement can be obtained by assuming a charge density of the order of 30% to 50% of the analytical values. The unphysical results are not unanticipated because the mean spherical approximation (MSA) assumes a weak interparticle interaction, as was discussed by Schmitz [54]. Even if good agreement was obtained by adjusting the charge number, it would not prove the RMSA concept. Table II shows that the σ_e/σ_a is between 0.5 and 0.05 for the univalent counterions and between 0.1 and 0.01 for the bivalent cases. Thus the 30 to 50% reduction of the charge number to reach the agreement appears to suggest that more refinement of the RMSA model is necessary.

V. CONCLUSION

We made SAXS measurements for aqueous solutions of PAMAM dendrimers with three generations (G4, G7, and G10), and SAXS curves could be described by theoretical values of the particle scattering function of an isolated sphere. Especially, the shape distributions of higher generation dendrimers were found to be narrow because of the jamming of end groups. Furthermore, radii of those dendrimers in acid solutions were a little larger than those in water.

For SAXS curves of univalent acid solutions, single scattering peaks were observed. The peak positions were dependent on the dendrimer concentration, indicating that those were due to the interparticle interaction. However, for $0.3<\alpha<0.8$, the position was independent not only of the acid concentration but also the counterion species. The effective charge density of the dendrimer determined by conductivity measurements was found to be insensitive to the acid concentration and the counterion species. $2D_{\mathrm{exp}}$ calculated from the peak position of the structure factor of G7 and G10 were obviously smaller, though slightly, than $2D_0$ calculated from molecular weights and concentrations of dendrimers, implying that acid solutions of dendrimers formed the two-state structures by the interparticle attractive force. However, in the USAXS curve for the hydrochloric acid solution, an upturn, which indicates the existence of structural inhomogeneities such as localized ordered structures, was not observed, probably due to the weak attraction and hence less clear distinction of the ordered and disordered regions. Furthermore, the difference between $2D_{\mathrm{exp}}$ and $2D_0$ increased with increasing generation, because of increasing effective charge number of a dendrimer particle and hence the enhanced interparticle interaction.

For sulfuric acid solutions, clear scattering peaks were not observed. The bivalent counterions were more strongly associated with the dendrimer ions than those for univalent ones. The charge neutralization took place more extensively for the bivalent ions than for the univalent counterions. The resulting low charge number of the dendrimers with the bivalent counterion was confirmed directly by the conductivity measurements. This observation confirms that the counterion-mediated attraction does exist with the univalent counterions and indicates the partial inappropriateness of frequent claims that the attraction is simply intensified with bivalent counterions. Finally, attention was drawn to the observation that the intensity of the counterion-mediated attraction in dendrimer solutions is determined by both the effective charge density and the effective charge number, in contrast with macroionic solutions or colloidal dispersions in which the charge density was an important factor.

ACKNOWLEDGMENT

We thank Dr. D. E. Valachovic for kindly sending her Ph.D. thesis.

[1] N. Ise, T. Okubo, Y. Hiragi, H. Kawai, T. Hashimoto, M. Fujimura, A. Nakajima, and H. Hayashi, J. Am. Chem. Soc. **101**, 5836 (1979).
[2] H. Matsuoka and N. Ise, Adv. Polym. Sci. **114**, 189 (1994).
[3] J. P. Moan and M. Moan, J. Phys. (Paris) **37**, 75 (1976).
[4] N. Ise, T. Okubo, K. Yamamoto, H. Kawai, T. Hashimoto, M. Fujimura, and Y. Hiragi, J. Am. Chem. Soc. **102**, 7901 (1980).
[5] K. S. Schmitz, M. Lu, and J. Gauntt, J. Chem. Phys. **78**, 5059 (1983).
[6] N. Ise, T. Okubo, M. Sugimura, K. Ito, and H. J. Nolte, J. Chem. Phys. **78**, 536 (1983).
[7] K. Ito, H. Nakamura, H. Yoshida, and N. Ise, J. Am. Chem. Soc. **110**, 6955 (1988).
[8] A. E. Larsen and D. G. Grier, Nature (London) **385**, 230 (1997).
[9] R. Kesavamoorthy and A. K. Arora, J. Phys. A **18**, 3389 (1985).
[10] H. Yoshida, N. Ise, and T. Hashimoto, J. Chem. Phys. **103**, 10146 (1995).
[11] F. Gröhn and M. Antonietti, Macromolecules **33**, 5938 (2000).
[12] D. A. Tomalia, H. Baker, J. Dewald, M. Hall, G. Kallos, S. Martin, J. Roeck, J. Ryder, and P. Smith, Polym. J. (Tokyo) **17**, 117 (1985).
[13] O. A. Matthews, A. N. Shipway, and J. F. Stoddart, Prog. Polym. Sci. **23**, 1 (1998).
[14] J. F. G. A. Jansen, E. M. M. de Brabander-van den Berg, and E. W. Meijer, Science **266**, 1226 (1994).
[15] R. Delong, K. Stephenson, T. Loftus, M. Fisher, S. Alahari, A. Nolting, and R. L. Juliano, J. Pharm. Sci. **86**, 762 (1997).
[16] H. Yoo, P. Sazani, and R. L. Juliano, Pharm. Res. **16**, 1799 (1999).
[17] P. W. Schmidt, Acta Crystallogr. **19**, 938 (1965).
[18] J. A. Lake, Acta Crystallogr. **23**, 191 (1967).
[19] T. Konishi, N. Ise, H. Matsuoka, H. Yamaoka, I. S. Sogami, and T. Yoshiyama, Phys. Rev. B **51**, 3914 (1995).
[20] J. Yamanaka, Y. Hayashi, N. Ise, and T. Yamaguchi, Phys. Rev. E **55**, 3028 (1997).
[21] G. Nisato, R. Ivkov, and E. J. Amis, Macromolecules **32**, 5895 (1999).
[22] D. E. Valachovic, Ph.D. thesis, University of Southern California, 1997.
[23] P. Welch and M. Muthukumar, Macromolecules **31**, 5892 (1998).
[24] N. Ise, Angew. Chem. Int. Ed. Engl. **25**, 323 (1986).
[25] S. Dosho, N. Ise, K. Ito, S. Iwai, H. Kitano, H. Nakamura, H. Okumura, T. Ono, I. Sogami, Y. Ueno, H. Yoshida, and T. Yoshiyama, Langmuir **9**, 394 (1993).
[26] N. Ise, T. Konishi, and B. V. R. Tata, Langmuir **15**, 4176 (1999).
[27] R. P. Feynman, R. B. Leighton, and M. Sands, *The Feynman Lecture on Physics* (Addison-Wesley, Reading, MA, 1963), Vol. 1, Chap. 2, pp. 2,3.
[28] This axiomatic situation arises from the fact that all ionic systems satisfy the electric neutrality principle. In other words, macroions alone cannot exist in solutions. When we say that like-charged macroions or particles attract each other through the intermediary of their counterions, the Coulomb law, that likes repel each other and unlikes attract, is not questioned. On the basis of this axiom, it is clear that, whether explicitly or not, any reasonable theories must be consistent with the existence of the counterion-mediated attraction, as was the case with the Debye-Hückel theory. The DLVO theory, which predicts the presence of electrostatic repulsion between particles only, is inconsistent with the axiom. This result originates from the improper treatment of the interparticle interaction, as demonstrated by the inconsistency of the DLVO theory with the Gibbs-Duhem relationship.
[29] K. S. Schmitz, *Macroions in Solution and Colloidal Suspension* (VCH, New York, 1993), Chap. 4.
[30] Because of the fact that the observed intraparticle scattering function $P(q)$ is sensitive to the solvent conditions as is observed in Fig. 2, it is less appropriate to use observed $P(q)$ that should be obtained from observed scattering functions at different solvent conditions with various concentrations of dendrimer and salt than to use calculated one. Though the calculated $P(q)$ is very different from observed $P(q)$ at large q, and then, the calculated $S(q)$ at large q is not true structure factor, the monotonic and smooth calculated $P(q)$ at low q calculated for uniform sphere may give sufficiently reliable first peak position in the resultant $S(q)$ obtained by Eq. (2).
[31] K. Ito, H. Okumura, H. Yoshida, Y. Ueno, and N. Ise, Phys. Rev. B **38**, 10852 (1988).
[32] H. Matsuoka, H. Tanaka, T. Hashimoto, and N. Ise, Phys. Rev. B **36**, 1754 (1987).
[33] H. Matsuoka, H. Tanaka, N. Iizuka, T. Hashimoto, and N. Ise, Phys. Rev. B **41**, 3584 (1990).
[34] H. Matsuoka, D. Schwahn, and N. Ise, Macromolecules **24**, 4227 (1991).
[35] J. Yamanaka, H. Yoshida, T. Koga, N. Ise, and T. Hashimoto, Phys. Rev. Lett. **80**, 5806 (1998).
[36] B. V. R. Tata and N. Ise, Phys. Rev. E **58**, 2237 (1998).
[37] R. Huizenga, P. F. Grieger, and F. T. Wall, J. Am. Chem. Soc. **72**, 2636 (1950).
[38] K. Ito, N. Ise, and T. Okubo, J. Chem. Phys. **82**, 5732 (1985).
[39] J. Th. G. Overbeek, Faraday Discuss. Chem. Soc. **90**, 183 (1990).
[40] V. Lobaskin, A. Lyubartsev, and P. Linse, Phys. Rev. E **63**, 020401(R) (2001).
[41] For a convenient review of our work in the early 1980s on polyelectrolyte, see Ref. [24].
[42] M. Drifford and J. P. Dalbiez, Biopolymers **24**, 1501 (1985).
[43] P. Wissenberg, T. Odijk, P. Cirkel, and M. Mandel, Macromolecules **28**, 2315 (1995).
[44] M. Sedlak and E. J. Amis, J. Chem. Phys. **96**, 817 (1992).
[45] M. Sedlak and E. J. Amis, J. Chem. Phys. **96**, 826 (1992).
[46] M. Sedlak, Macromolecules **26**, 1158 (1993).
[47] M. Sedlak, J. Chem. Phys. **105**, 10123 (1996).
[48] B. D. Ermi and E. J. Amis, Macromolecules **29**, 2701 (1996).
[49] W. Nierling and E. Nordmeir, Polym. J. (Tokyo) **29**, 795 (1997).
[50] R. Borsali, H. Nguyen, and R. Pecora, Macromolecules **31**, 1548 (1998).
[51] B. D. Ermi and E. J. Amis, Macromolecules **31**, 7378 (1998).
[52] J. Ray and G. S. Manning, Macromolecules **33**, 2901 (2000).
[53] J. Yamanaka *et al.* (in preparation).
[54] See Ref. [29], Chap. 2.